COMPUTATIONAL
AND STRUCTURAL
BIOTECHNOLOGY
J O U R N A L

De novo genome assembly of the potent medicinal plant *Rehmannia glutinosa* using nanopore technology

Ligang Ma [a,b,1], Chengming Dong [a,b,1], Chi Song [c,1], Xiaolan Wang [a,b,1], Xiaoke Zheng [a,b], Yan Niu [d], Shilin Chen [c,*], Weisheng Feng [a,b,*]

[a] *College of Pharmacy, Henan University of Chinese Medicine, Zhengzhou 450046, China*
[b] *Co-construction Collaborative Innovation Center for Chinese Medicine and Respiratory Diseases by Henan & Education Ministry of P.R. China, Zhengzhou 450046, China*
[c] *Key Laboratory of Beijing for Identification and Safety Evaluation of Chinese Medicine, Institute of Chinese Materia Medica, China Academy of Chinese Medical Sciences, Beijing 100700, China*
[d] *Wuhan Benagen Tech Solutions Company Limited, Wuhan 430070, China*

A R T I C L E   I N F O

A B S T R A C T

Rehmannia glutinosa is a potent medicinal plant with a significant importance in traditional Chinese medicine. Its root is enriched with various bioactive molecules mainly iridoids, possessing important pharmaceutical properties. However, the molecular biology and evolution of *R. glutinosa* have been largely unexplored. Here, we report a reference genome of *R. glutinosa* using Nanopore technology, Illumina and Hi-C sequencing. The assembly genome is 2.49 Gb long with a scaffold N50 length of 70 Mb and high heterozygosity (2%). Since *R. glutinosa* is an autotetraploid (4n = 56), the difference between each set of chromosomes is very small, and it is difficult to distinguish the two sets of chromosomes using Hi-C. Hence, only one set of the genome size was mounted to the chromosome level. Scaffolds covering 52.61% of the assembled genome were anchored on 14 pseudochromosomes. Over 67% of the genome consists of repetitive sequences dominated by *Copia* long terminal repeats and 48,475 protein-coding genes were predicted. Phylogenetic analysis corroborates the placement of *R. glutinosa* in the Orobanchaceae family. Our results indicated an independent and very recent whole genome duplication event that occurred 3.64 million year ago in the *R. glutinosa* lineage. Comparative genomics analysis demonstrated expansion of the UDP-dependent glycosyltransferases and terpene synthase gene families, known to be involved in terpenoid biosynthesis and diversification. Furthermore, the molecular biosynthetic pathway of iridoids has been clarified in this work. Collectively, the generated reference genome of *R. glutinosa* will facilitate discovery and development of important pharmacological compounds.

1. Introduction

Plants are source of rich natural products representing tremendous resources for drug development. There are over 200,000 plant secondary metabolites known to date with several compounds heavily used as drugs [1]. Besides their applications in drug discovery, plants are exploited by human for centuries as herbal drugs and traditional knowledge of plant-based therapies have been transmitted from generation to generation. Population in India, China, Japan, Korea and several African and South American countries considerably rely on traditional herbal medicine [2]. Among the 21,000 medicinal plants listed by the World Health Organization, *Rehmannia glutinosa* Libosch. Ex Fisch. & C.A. Mey represents one of the most important. It is widely cultivated in Asian countries such as China, Korea, Japan and Vietnam. *R. glutinosa* has been listed as one of the 50 fundamental herbs in traditional Chinese medicine [3]. It plays a wide range of long lasting pharmacological activities on human health with very less side effects [4]. The main medicinal tissue of *R. glutinosa* is the tuberous root (Fig. 1), which is used for the treatment of heat and strengthening body tonicity. It has also significant effects on the cardiovascular system, central nervous system, immune system, and visceral system based on in-vitro assays [4–10].

Several bioactive compounds with important pharmaceutical activities have been reported in *R. glutinosa* root including iridoids (catalpol, rehmannioside A, B, C and D, geniposide, aucubin),

* Corresponding authors at: College of Pharmacy, Henan University of Chinese Medicine, Zhengzhou 450046, China (W. Feng).

E-mail addresses: slchen@icmm.ac.cn (S. Chen), fwsh@hactcm.edu.cn (W. Feng).
[1] Co-first authors.

Fig. 1. Phenotype of *Rhemannia glutinosa* cultivar Qinhuai used in this study. Left: whole plant in flowering stage, Right above: leaf, Right below: tuberous root. Scale = 1 cm.

ionones and phenylethanoids [3,4,11,12]. Despite the beneficial properties of these bioactive compounds, the molecular mechanisms of their formation are yet to be elucidated mainly because of the lack of high-quality genome resources in *R. glutinosa* [13–17].

The exact phylogenetic placement of *R. glutinosa* in the Lamiales order has been elusive. Initially, based on morphological traits it was placed in the Scrophulariaceae family but after several revisions, it has been classified as a species of the Orobanchaceae family [18–21]. Nonetheless, the genome structure and evolution of *R. glutinosa* is yet to be elucidated.

Sequencing and investigating genome evolution in medicinal plants is essential for elucidating their phylogenetic relationship, promoting their sustainable exploitation and facilitating plant-based drug discovery [22]. Genome sequences of several species in the Lamiales order are now available [23–28], which will facilitate comparative evolutionary studies in *R. glutinosa*. Recently, the rapid development in new sequencing technologies (Oxford Nanopore Technologies (ONT), PacBio sequencing) and complementary long-range scaffolding technologies (Hi-C sequencing and Bionano optical maps) have facilitated the generation of chromosome-scale genome assemblies in various plant species with large and complex genomes [29,30].

In this report, we *de novo* sequenced and assembled a reference genome of *R. glutinosa* by combining ONT long reads, Illumina NovaSeq short reads and Hi-C sequencing. We annotated and characterized the structure and evolutionary history of the large and complex genome of *R. glutinosa*. We further performed a genome-wide prediction and expression analysis of terpene synthase and UDP-dependent glycosyltransferases gene families known to be involved in the biosynthesis and diversification of terpenoids. Our work elucidates the genomic evolution of *R. glutinosa* and provides essential genomic resources for decoding the synthetic pathways of bioactive compounds to facilitate molecular breeding of cultivars with improved medicinal attributes.

2. Material and methods

2.1. Plant materials, DNA library construction and sequencing

Rehmannia glutinosa Libosch. Ex Fisch. & C.A. Mey cultivar Qinhuai is one of the ten main cultivars grown in China. Qinhuai is rich in catalpol, verbascoside, iridoids, and is mainly grown in Jiaozuo, Daohuang district, Henan province, China. Healthy tissue-cultured plants of Qinhuai were obtained from the College of Pharmacy, Henan University of Chinese Medicine, China. High-quality genomic DNA was isolated from fresh leaves using the conventional cetyltriethylammonium bromide method [31]. Agarose gel electrophoresis was used to check the integrity of DNA (DNA Integrity Number > 8) /RNA (RNA Integrity Number > 6). In order to obtain longer reads, it is generally necessary to screen large fragment sequences through gel cutting instead of sequence fragmentation. Illumina sequencing pair-end libraries with insert size of 150 bp were prepared using Nextera DNA Flex Library Prep Kit (Illumina, San Diego, CA, USA). Sequencing was performed using the Illumina NovaSeq platform (Illumina, San Diego, CA, USA). Raw reads (170.32 Gb) were cleaned to discard low-quality reads (reads with adaptors and unknown nucleotides and reads with>20% low-quality bases) using the FastQC (v.0.11.8) tool (https://www.bioinformatics.babraham.ac.uk/projects/fastqc/) and, after data filtering, 157.73 Gb clean data were used for subsequent analyses (Table S1).

For Oxford Nanopore sequencing, the libraries were prepared with the standard protocol from Oxford Nanopore Technologies previously detailed by Song et al. [32]. The purified library was loaded onto primed R9.4 Spot-On Flow Cells and sequenced using a PromethION sequencer (Oxford Nanopore Technologies, Oxford, UK) with 48-h runs at Wuhan Benagen Tech Solutions Company Limited, Wuhan, China. Base calling analysis of raw data was performed using the Oxford Nanopore GUPPY software (v0.3.0). A total of 297.86 Gb raw data was generated with 230.83 Gb 'passed' reads after quality control.

2.2. RNA library construction, sequencing and data processing

Total RNA was extracted from young leaves, mature leaves, jasmonic acid-treated leaves and roots, salicylic acid-treated leaves and roots of cultivars Qinhuai, Huaifeng and Wen85-5 using the HiPure Plant RNA Kit according to the manufacturer's instructions (Magen, Guangzhou, China). RNA samples were pooled and used for library preparation following the standard protocol from Oxford Nanopore Technologies with the library prep kit (SQK-PC S109 + SQK-PBK004). The library was loaded onto R9.4 SpotON Flow Cells (Oxford Nanopore Technologies, Oxford, UK) and sequenced using a 48-h run time. In addition, Illumina RNA-seq (Illumina NovaSeq, San Diego, CA, USA) short reads were generated based on tissue culture seedlings (triplicate samples) from the cultivars Huaifeng and Qinhuai. RNA-seq reads were remapped to the reference genome assembly using STAR (v.2.7.0; parameters: --twopassMode None) [33] and the FPKM was calculated to evaluate the expression level of each gene using the RSEM (v.1.2.15) tool [34].

2.3. Genome assembly

Based on the sequencing data, the K-mer analysis method [35] was used to estimate the genome size and heterozygosity using the kmer_freq program in the gce package (v.1.0.0) [36]. Genomic assembly was performed using SMARTdenovo software (https://github.com/ruanjue/smartdenovo; parameter: -p jvh -k 17 -J 2000 -t 32 -c 1). Two rounds of error correction were performed on the assembly result based on the Nanopore sequencing data using Racon (v.1.4.11) (https://github.com/isovic/racon). Two rounds of error correction were performed on the assembly result based on the Illumina Novaseq sequencing data using Pilon (v.1.22; parameters: default) [37]. Finally, the genome was de-hybridized using the Purge_haplotigs pipeline (v.1.0.4) [38] to obtain the final assembly result.

2.4. Pseudochromosome level assembly using Hi-C

High-quality DNA extracted from young leaves of healthy tissue-cultured plants was used for Hi-C sequencing. Formaldehyde was used for fixing chromatin. *In situ* Hi-C chromosome conformation capture was performed according the DNase-based protocol described by Ramani et al. [39]. The libraries were sequenced using 350 bp paired-end mode on an Illumina NovaSeq (Illumina, San Diego, CA, USA). For pseudochromosome level scaffolding, we used the assembly software ALLHIC (v. 0.9.12) [40] and 3D-DNA (v.180419) [41] for stitching, and then we imported the final files (.hic and .assembly) generated by the software into Juicebox (v1.11.08) [42] for plotting.

2.5. Genome annotation

2.5.1. a) repeat sequence annotation

We used the RepeatModeler (v.1.0.4) (https://github.com/rmhubley/RepeatModeler) software to build our own repeat library. After merging the repbase library, we used RepeatMasker (v.4.0.5) (http://www.repeatmasker.org/) for genome repeat annotation.

2.5.2. b) gene prediction

Gene prediction was performed using MAKER software (v.2.31.8) [43] and Augustus software (v.3.0.3) [44]. Protein coding sequences from 15 species including, *Cuscuta australis*, *Ipomea nil*, *Capsicum annuum*, *Solanum melongena*, *Solanum lycopersicum*, *Chrysanthenum nankingense*, *Helianthus annuus*, *Sesamum indicum*, *Erythranthe guttata*, *Olea europeae* subsp. *sylvestris*, *Utricularia*

gibba, *Antirrhinum majus*, *Arabidopsis thaliana*, *Oryza sativa* and *Vitis vinifera* (Table S2), were mapped to the assembly of *R. glutinosa* using BLAST (v.2.6.0+; parameter: -evalue 1e-5) [45]. The predicted genes were corrected with the *de novo* assembled RNA-seq long and short reads using Trinity (v.2.6.6) [46]. Next, we employed the BUSCO software (v.4.1.2) [47] for evaluating the quality of the prediction based on the eukaryotic database.

2.5.3. c) gene function annotation

Using BLAST (v.2.6.0+; parameters: -evalue 1e-5 -max_target_seqs 5 -num_threads 10) [45], the predicted protein sequences were compared with the transposable element (TE) protein library. After removing the TE protein genes, the protein-coding genes were functionally annotated based on seven publicly available databases including, Uniprot [48], Pfam [49], GO [50], KEGG [51], Swissprot [48], Interpro [52] and NR [53].

2.5.4. d) Non-coding RNA annotation

Based on the structural features of tRNA, tRNAscan-SE (v.1.23) [54] was used to find tRNA sequences in the *R. glutinosa* genome. Furthermore, rRNA prediction was performed using RNAmmer (v.1.2) [55]. The miRNA and snRNA was predicted using Rfam_scan.pl (v1.0.4) by inner calling using Infernal (v1.1.1) [56].

2.6. Gene family and evolutionary analysis

2.6.1. a) Gene family clustering

All amino acid sequences of the 15 selected species in addition to *R. glutniosa* were aligned using BLASTP (v.2.6.0; parameters: -evalue 1e-5 -outfmt 6) [45], and the gene family clustering was performed using OrthoMCL software (v.2.0.9; parameters: percentMatchCutoff = 30, evalueExponentCutoff = 1e-5, expansion coefficient 1.5) [57].

2.6.2. b) Phylogenetic tree construction

A single copy gene family shared by the 16 selected species was screened to construct a phylogenetic tree. First, the protein sequence of each single copy gene family was subjected to alignments in MUSCLE (v.3.8.31) [58] and finally, the maximum likelihood tree was built using RAxML (v.8.2.10) software [59].

2.6.3. c) Gene family contraction and expansion

Gene family contraction and expansion analysis was performed using CAFÉ (v.2.1; parameter: --filter) software [60] based on gene family clustering results.

2.6.4. d) Divergence time analysis

Based on the phylogenetic tree result, the mcmctree of PAML (v.4.9) (parameters: nsample = 1000000; burnin = 200000; seqtype = 0; model = 4) [61] was used to estimate the differentiation time of the different species. Published divergence times for *Vitis vinifera-Oryza sativa*: 125–150 million years ago (Mya) and *Solanum lycopersicum-Helianthus annuus*: 95–106 Mya were used to calibrate the divergence time.

2.6.5. e) Whole gene duplication analysis

Whole genome duplication analysis was performed based on five species: *Solanum lycopersicum*, *Cuscuta australis*, *Ipomoea nil*, *Vitis vinifera* and *R. glutinosa*. First, we compared the protein sequences of different species using the all-to-all search in BLASTP (v.2.6.0+; parameters: -evalue 1e-5 -outfmt 6) [45], and then used MCScanX (https://github.com/wyp1125/MCScanx; parameters: -a -e 1e-5 -s 5) [62] to analyze the genomic collinear block, and finally calculate the synonymous mutation frequency (Ks) of the collinear gene pairs based on the NG method of Yang implemented in PAML (v.4.9) [61]. The synonymous mutation rate distribution (Ks) was

plotted using ggplot2 (v.2.2.1) package in R v.2.15 (www.r-project.org). The synonymous substitution rate of 8.25 X 10^{-9} mutations per site per year was applied to calculate the ages of the WGDs.

2.7. Investigations of terpene synthase (TPS), UDP-dependent glycosyltransferase (UGT) and iridoid biosynthetic pathway associated genes

The Hidden Markov Model profiles of the TPS domains (PF01397 and PF03936) and UGT domain (PF00201) were obtained from Pfam v.32.0 database (http://Pfam.sanger.ac.uk/) [63] and searched against the genomes of *R. glutinosa* and related species using HMMER V.3.0 program with "trusted cutoff" as threshold [64]. Candidate genes were further confirmed using the SMART tool [65]. Redundant sequences and sequences without conserved motifs were removed. TPS genes were grouped into subfamilies according to Chen et al. [66]. Similarly, UGT genes were assigned to different families based on the previous work of Yonekura-Sakakibara and Hanada [67]. The protein sequences of genes were subjected to alignments in MUSCLE (v.3.8.31) [58] and the maximum likelihood tree was built using RAxML (v.8.2.10) software [59].

Iridoids are derived from either the plastidial 2-C-methyl-d-erythritol-4-phosphate (MEP) pathway or the cytosolic mevalonic acid (MVA) pathway. Using the KEGG annotation, we searched for all genes MEP and MVA pathways genes and reconstructed the iridoids biosynthesis pathway [11,68]. Heatmaps displaying gene expression profiles were plotted using pheatmap (v.1.0.12) in R v.2.15 (www.r-project.org) based on various RNA-seq data (Table S3).

3. Results and discussion

3.1. Genome sequencing and assembly

In order to estimate the genome size and heterozygosity of *Rehmannia glutinosa* cultivar 'Qinhuai', genome survey sequencing was performed. A total of 170.32 Gb of Illumina NovaSeq reads was generated and the estimated genome size was 2.35 Gb according to the 19-mer depth distribution (Table S4, Figure S1). Compared to other genome sequenced plant species in the Lamiales order (*Sesamum indicum*, *Erythranthe guttata*, *Olea europeae* subsp. *sylvestris*, Olea europaea subsp. europaea, *Salvia splendens*, *Utricularia gibba*, *Antirrhinum majus*, *Scutellaria baicalensis*), *R. glutinosa* features the largest genome [23–28,69]. High heterozygosity (2%) was estimated in *R. glutinosa* genome and the 19-mer distribution indicated a large proportion of repeat sequences (Table S4), denoting a challenging *de novo* genome assembly of this species [70].

The hybrid sequencing approach combining long reads and short reads technologies has proven to be efficient for plant species with large or complex genome [32,69,71,72]. Here, we also employed a hybrid genome sequencing approach by combining Oxford Nanopore Technologies (ONT) and Illumina NovaSeq platform (Figure S2). The ONT yielded 297.86 Gb raw data from 3 flow cells composed of 14 million reads (read N50 length, 28.5 Kb) (Table S5). After data filtering (remove reads of quality score < 7), 230.82 Gb data were kept for downstream analyses, representing 98-fold genome coverage (Table S5). A total of 157.73 Gb Illumina clean reads were generated (Table S1), representing 67-fold genome coverage. The genome assembly was conducted on a computer with 250 G CPU memory and 80 threads (Table S6). We assembled and corrected the Nanopore long reads prior using Illumina reads for polishing. In addition, Hi-C data were used for scaffold extension and chromosome mount. Globally, the final assembled genome had a total length of 2.49 Gb and a contig

N50 of 658 Kb (Table 1). The assembled genome size is slightly larger than the estimated size of 2.35 Gb, probably due to the high heterozygosity. Similar observations were previously reported in Olea europaea subsp. europaea and *Carya illinoinensis* [25,73]. In *de novo* genome sequencing, the application of Hi-C scaffolding facilitates sequence continuity to reach a chromosome scale [74]. Since *R. glutinosa* is an autotetraploid (4n = 56) [75], the difference between each set of chromosomes is very small, and it is difficult to distinguish the two sets of chromosomes using Hi-C. Hence, only one set of the genome size was assembled to the chromosome level. Herein, Hi-C assisted assembly helped to anchor a total of 52.61% of *R. glutinosa* genome on 14 pseudochromosomes named as chr1 ~ chr14 (Fig. 2A, Figure S3, Table S6, Table S7, Table S8), which is consistent with the karyotype (4n = 56) previously reported by Xu [75]. We aligned the Illumina short reads to the assembled genome using BWA, resulting in a mapping rate of 93.7%.

3.2. Gene annotation

Analysis of the repeat sequences in Qinhuai genome revealed over 67% repetitive sequences, with the dominant type (>75%) being transposable elements (TE) (Table S9). This is higher than the 29, 43, 55, 58% of repeat sequences reported in genomes of sesame, *Olea europeae* subsp. *sylvestris*, *Antirrhinum majus* and *Salvia splendens* [24,26–28]. TEs could be roughly classified into four types: long terminal repeat (LTR), long interspersed nuclear element, short interspersed nuclear element and DNA transposons. We found that LTRs represent the major repetitive sequences (45%). It has been evidenced that abundance of LTRs contributes to genome size expansion in plants with varying proportions of LTR superfamilies' [76]. For instance, higher *Gypsy* than *Copia* elements was observed in cowpea, *Salvia splendens*, walnut, *Polygonum cuspidatum* and Helianthus *annus* [27,72,77–79]. On the opposite, in plant species such as tomato, *Chrysanthemum nankingense* and sesame, *Copia* elements are more dominant than *Gypsy* elements [24,32,80]. In the present study, we noticed that *Gypsy* elements and *Copia* elements contribute to 13% and 31% in the genome, respectively (Table S9), implying that the large genome size of *R. glutinosa* is mainly attributable to the amount of *Copia* retrotransposons.

An integrated gene prediction protocol was employed based on a combination of *de novo* assembly of transcriptomes from various cultivars, tissues and stress conditions (whole seedlings (Qinhuai, Wen85-5 and Huaifeng cultivars), young leaves, mature leaves, jasmonic acid-treated leaves and roots, salicylic acid-treated leaves and roots (Table S3), *ab initio* prediction and homology search with protein sequences from 16 related species. In total, 48,475 protein-coding genes were obtained in *R. glutinosa* genome with an average mRNA length, coding sequence length and exon number of 5.01 Kb, 1,291.21 bp and 5.89 per gene, respectively (Table S10). The predicted gene was evaluated based on the embryophyta database using the BUSCO software [47], which delivered a score of completeness of 97.83% including complete and fragmented BUSCOs (Table S11). This result suggests that a near completion genome sequence has been generated for *R. glutinosa* in this study, similar to published genomes of Arabidopsis and rice [81,82]. A total of 48,475 protein-coding genes were obtained in *R. glutinosa* genome, ranking this species as the most gene-enriched in the Lamiales order. Nonetheless, it is worth mentioning that the number of predicted genes can enormously vary depending on the tools and parameters used in gene prediction. We obtained 99% of the predicted protein-coding genes matching entries in seven publicly available databases (Table S12). With regard to non-coding genes, we identified 351 miRNA, 1,800 tRNA,

Table 1
Summary of *R. glutinosa* genome assembly.

Genome features	Contig	Scaffold
Total_length (bp)	2,498,530,510	2,498,814,810
Number of contigs	5,290	3,733
GC_content (%)	36.52	36.52
N50 (bp)	658,887	70,280,146
N90 (bp)	244,881	262,126
Average (bp)	472,312.01	669,385.16
Median (bp)	363,729	239,898
Min (bp)	30,576	25,000
Max (bp)	2,924,441	166,779,478

1,199 rRNA and 2,945 snRNA fragments from the total assembly (Table S13).

3.3. Gene family and phylogenetic analysis

The genome assembly for *R. glutinosa* was compared with 15 genome-sequenced plant species, including five Solanales species (*Cuscuta australis*, Convolvulaceae; *Ipomea nil* Convolvulaceae; *Capsicum annuum*, Solanaceae; *Solanum melongena*, Solanaceae; *Solanum lycopersicum*, Solanaceae), two Asterales species (*Chrysanthenum nankingense*, Asteraceae; *Helianthus annuus*, Asteraceae), five Lamiales species (*Sesamum indicum*, Pedaliaceae; *Erythranthe guttata*, Prhymaceae; *Olea europeae* subsp. *sylvestris*, Oleaceae; *Utricularia gibba*, Lentibulariaceae; *Antirrhinum majus*, Plantaginaceae), one Brassicales species (*Arabidopsis thaliana*, Brassicaceae), one Poales species (*Oryza sativa*, Poaceae), and one Vitales species (*Vitis vinifera*, Vitaceae) (Table S2). Based on gene family clustering analysis, 44,335 gene families (689,787 genes) were detected, including 5,309 core gene families (126,451 genes) shared by all the 16 species and 12,380 gene families shared by the four Lamiales species (Fig. 2B; Table S14). Specific genes found in *R. glutinosa* genome were enriched in various gene ontology (GO) functional categories with the most enriched being the general GO term GO:0016799 (hydrolase activity) and specific GO terms GO:0047938 (glucose-6-phosphate 1-epimerase activity), GO:0016114 (terpenoid biosynthetic process), GO:0047924 (geraniol dehydrogenase activity), GO:0046029 (mannitol dehydrogenase activity), suggesting a high enzymatic activity in *R. glutinosa* (Table S15).

We constructed a phylogenetic tree based on 266 gene families shared by all species as single-copy orthologous gene families
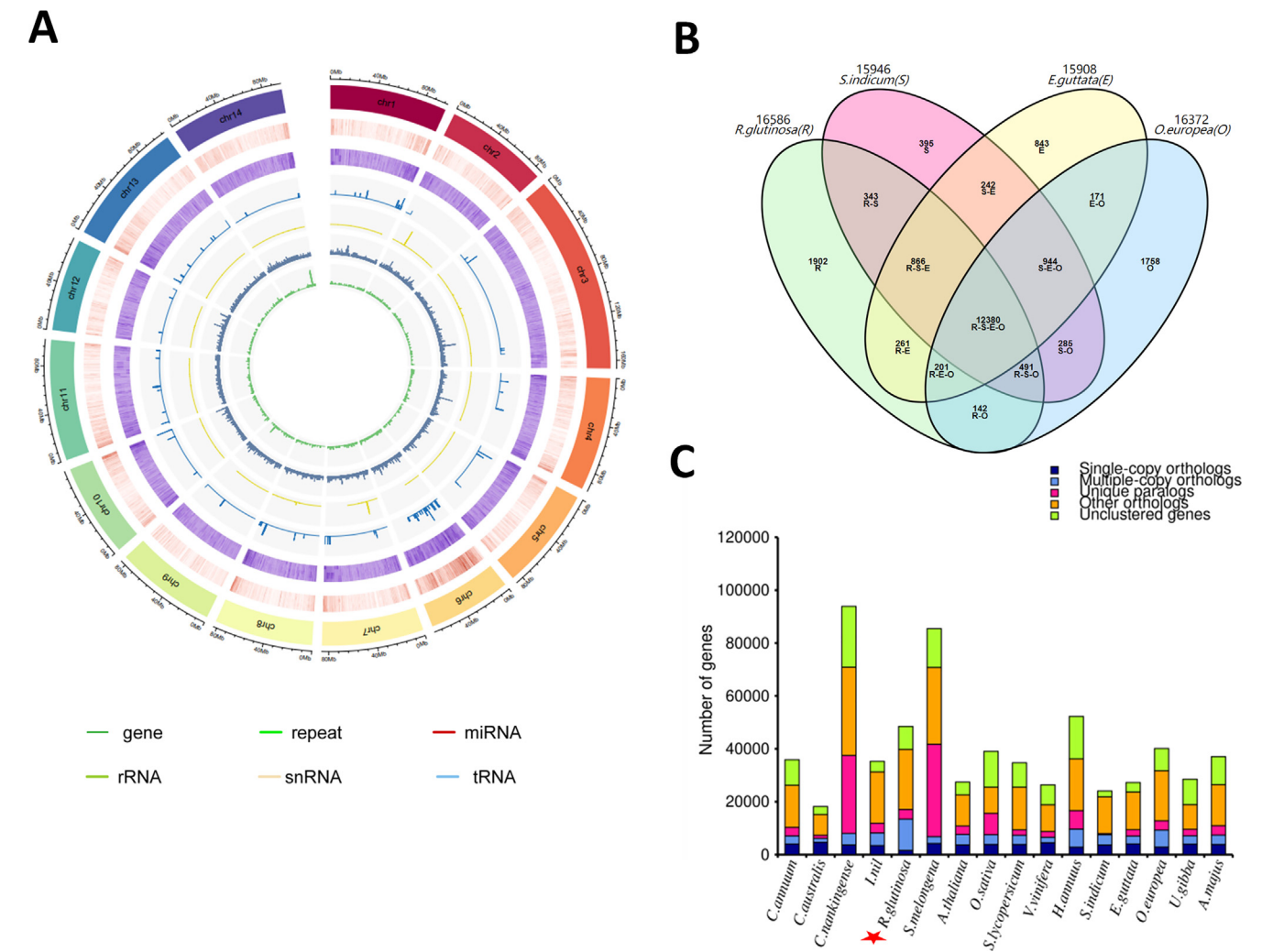

Fig. 2. *De novo* genome assembly of *R. glutinosa* and comparative analysis with related species. (A) Summary of the *de novo* genome assembly and sequencing analysis of *R. glutinosa* cultivar Qinhuai (from outside to inside: 1. pseudochromosome number; 2. gene density; 3. repeat density; 4. miRNA density; 5. rRNA density; 6. snRNA density; 7. tRNA density). (B) Venn diagram showing the shared and unique gene families among four Lamiales species. (C) Distribution of genes and gene families across 16 plant species. The red star marks the position of the sequenced species in this study. (For interpretation of the references to colour in this figure legend, the reader is referred to the web version of this article.)

(Fig. 2C). Our goal was to clarify whether *R. glutinosa* belongs to Scrophulariaceae or Orobanchaceae. Based on previous phylogenetic analyses, Scrophulariaceae and Plantaginaceae are closely related while Orobanchaceae is very close to Prhymaceae [16,28,83]. Therefore, we integrated *A. majus* (Plantaginaceae) and *E. guttata* (Prhymaceae) in our analysis. We found that *R. glutinosa* was clustered together with Lamiales species, which is consistent with its phylogenetic placement (Fig. 3). Remarkably, *E. guttata* was the closest species to *R. glutinosa*. Since Phrymaceae is close to Orobanchaceae, we deduce that *R. glutinosa* belongs well to the family of Orobanchaceae. The Orobanchaceae family is essentially composed of parasitic plant species [84,85]. Therefore, the integration of some non-parasitic plant species such as *R. glutinosa* in this family still needs further clarification. Recent progresses on genome sequencing of parasitic plants in Orobanchaceae family such as *Striga asiatica* [86] will be helpful to elucidate the genome evolution and systematics of this family.

R. glutinosa was estimated to have diverged from *E. guttata* 21.1 million years ago (Mya) and from the Solanales approximately 86.3 Mya (Fig. 3), which is in accordance with estimations that the Lamiales order has diverged from the Solanales order between 89.8 and 185.8 Mya [24]. Evolutionary driven modifications of gene family size are a natural phenomenon providing selective advantages and contributing to organizational and regulatory diversity in a variety of organisms [87,88]. In this study, we investigated the gene family expansion and contraction in *R. glutinosa* lineage. The analysis revealed that 6,237 gene families underwent expansion, while a significant number of gene families (848) underwent contraction (Fig. 3). Interestingly, the expanded gene families were mainly enriched in GO:0008299 (isoprenoid biosynthetic process) (Table S16), which may have contributed to the high content of bioactive metabolites in this important medicinal plant [4,89].

3.4. Whole genome duplication event

Whole-genome duplication (WGD) is a main causal agent in diversification, phenotypic and developmental innovation in organisms [90]. Novel lineage-specific WGD events have been reported and dated in all Lamiales species with published genomes. For example, sesame, *A. majus* and *E. europea* subsp. *sylvestris* experienced an independent WGD at 71, 46 and 28 Mya, respectively [24,26,28]. WGD event was examined in *R. glutinosa* in comparison with four other species (*Solanum lycopersicum*, *Cuscuta australis*, *Ipomoea nil* and *Vitis vinifera*). We identified the syntenic blocks within genomes through intragenome comparisons (Fig. 4A). There was a prominent peak for calculated synonymous substitution rates (Ks) of gene pairs at 0.06 in the *R. glutinosa* lineage (Fig. 4B), indicative of a very recent independent WGD event which occurred 3.64 Mya after splitting from *E. guttatus* (21.1 Mya) [91].

3.5. Molecular biosynthetic pathway of iridoids

The major bioactive molecule in R. glutinosa is iridoid [4,9]. It has been well documented that iridoids possess beneficial antitumor, antioxidant, diuretic, neuroprotective and anti-inflammatory effects on human health [5,92–94]. >30 kinds of iridoids have been isolated from *R. glutinosa* including, catalpol, aucubin, rehmannioside A, B, C and D [4]. Iridoids are monoterpenes and two general synthetic pathways of terpenoids biosynthesis have been recognized in plants: mevalonate pathway (MVP) and 2C-methyl-D-erythritol-4-phosphate pathway (MEP) [95]. Based on the extensive investigations on Catharanthus roseus and R. glutinosa, two main routes for iridoids biosynthesis have been proposed (Fig. 5A) [68,96,97], however structural genes catalyzing steps of this complex pathways have not yet been fully identified [11,98].

In this study, we searched for all genes involved in the iridoid biosynthesis pathway and identified a total of 313 candidate genes belonging to 25 enzyme families (Table S17). We employed transcriptome data from root and leaf tissues in order to identify key genes differentially expressed genes (DEG) between tissues and growth stages that could be target of further functional analyses. In total, 137 DEGs were detected and our analysis showed that most of them were up-regulated in older root samples (SP2: 1 month and SP3: 2 months after sprouting) as compared to young root samples (SP1: 15–20 days after sprouting). Duan et al. [98] reported that the content of iridoid in *R. glutinosa* root increased continuously during growth stages up to 2 months and this correlates well with the expression patterns of the identified DEGs in this study. Furthermore, by comparing expression patterns in root and leaf tissues, we observed that most of the DEGs were downexpressed in the leaf tissues, confirming the fact that iridoids are mainly enriched in *R. glutinosa* root [99]. Further studies aiming at identifying the transcription factors regulating these DEGs through gene co-expression network analysis [100], will provide important tools for increasing iridoid content not only in root but also in leaf.

3.6. Prediction and expression analysis of terpene synthase gene family

Terpene synthase (TPS) gene family members are key enzymes generating the huge variety of terpene structures [101]. We searched for all annotated TPS genes within *R. glutinosa* genome and compared with six other species (*A. thaliana*, *A. majus*, *C. australis*, *I. nil*, *S. lycopersicum* and *V. vinifera*). In total, 87 TPS genes were identified, largely surpassing the number of TPS members in other species (Table S18). This indicates an expansion of TPS gene family in *R. glutinosa* mainly the TPS-a and TPS-b subfamilies. Furthermore, a comparison with *A. thaliana* revealed several clusters of TPS genes unique to *R. glutinosa* (Fig. 5B), which may play preponderant role in iridoid biosynthesis. We analyzed the expression of TPS genes in various cultivars (Qinghuai, Wen85 and Huaifeng), growth periods (15–20 days, 1 month and 2 months after sprouting root), tissues (root and seedling), root parts (radial striation and non-radial striation) and salicylic acid (SA) treatments (Table S3). Overall, most of TPS genes were preferentially expressed in root tissues than in seedling, which correlates well with the higher content of iridoids in *R. glutinosa* root [99] (Figure S4). In addition, we found that SA treatment stimulates TPS gene expression and could contribute to high accumulation of iridoids [13]. Finally, we observed a variation of TPS gene expression among cultivars and growth periods (Figure S4), which may provide prospects for increasing iridoid content in *R. glutinosa* root [13,14].

3.7. Prediction and expression analysis of UDP-dependent glycosyltransferase gene family

Glycosylation represents the last step in the biosynthesis of numerous natural compounds, including terpenes [102,103]. In *R. glutinosa*, glycosylation plays a crucial role in iridoids biosynthesis since most of the iridoids are mainly present as glycosides [4,104]. UDP-dependent glycosyltransferases (UGTs) belong to the largest family of the glycosyltransferase superfamily and catalyzes glycosylation process [105]. We examined the UGT gene family in
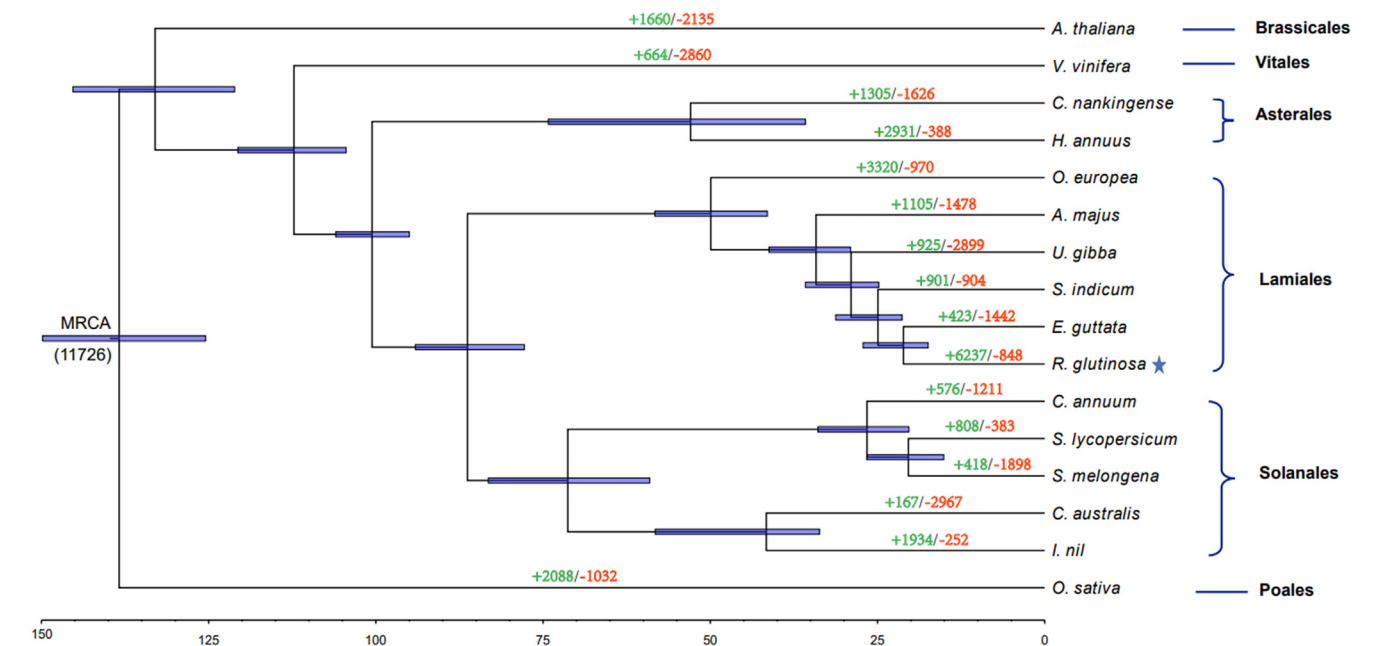
Fig. 3. Phylogenetic analysis and divergence time estimations among 16 plant species including *R. glutinosa*. The tree was constructed based on all single-copy orthologous genes using *Oryza sativa* as outgroup. A total of 500 bootstrap replicates was performed and bootstrap values lower than 100 are not presented. The star marks the species used for genome sequencing in this study. Divergence times estimated in million years ago are indicated by the blue lines over the nodes. The span of the blue lines shows 95% confidence interval of the divergence time. The divergence time was estimated for each node in million years (MY). The number of gene-family contraction and expansion events is indicated by green and red numbers, respectively. The number at the root (11,726) denotes the total number of gene families predicted in the most recent common ancestor (MRCA). (For interpretation of the references to colour in this figure legend, the reader is referred to the web version of this article.)
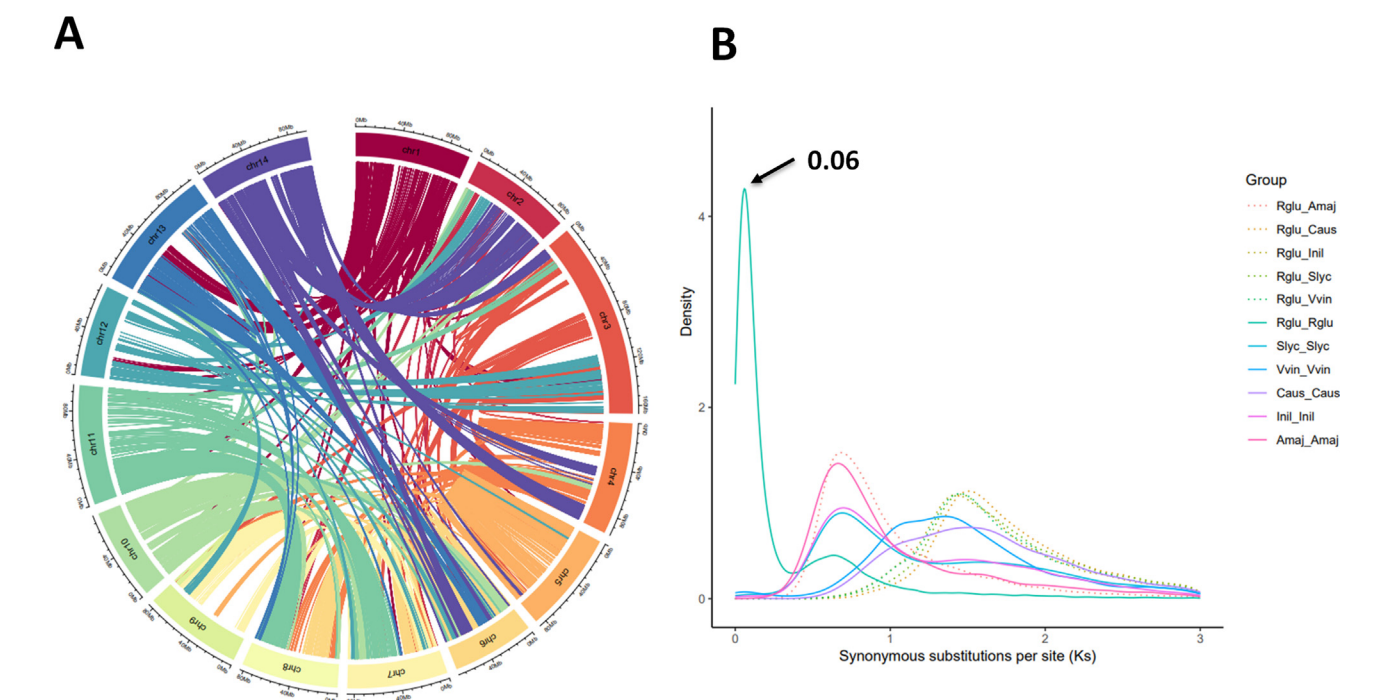
Fig. 4. Comparative genomic and evolutionary analysis. (A) Intragenome comparison showing syntenic relationship between *R. glutinosa* pseudochromosomes. (B) Distribution of synonymous substitution rates (Ks) for pairs of syntenic paralogs in *R. glutinosa* and four other species (Rglu: *Rhemannia glutinosa*, Slyc: *Solanum lycopersicum*, Caus: *Cuscuta australis*, Inil: *Ipomoea nil* and Vvin: *Vitis vinifera*).

R. glutinosa genome in comparison with *A. thaliana* and *V. vinifera*. In total, 333 UGT genes were detected in *R. glutinosa* with members of the groups A and G being the most dominant. Similar to TPS, we observed that UGT gene family has been expanded in *R. glutinosa* as its members were higher than *V. vinifera* and *A. thaliana* (Table S18;

Table S19; Fig. 5C). Gene expression profiling in root and seedling showed globally a tissue-preferential activity of UGTs in *R. glutinosa* (Figure S5). The UGTs highly active in root tissues represent important candidate gene resources for further functional analyses to uncover their specific roles in iridoid decoration.

Fig. 5. Genes involved in iridoids biosynthesis and glycosylation. (A) Biosynthesis pathways of iridoids in *R. glutinosa*. Log2 fold change of the differentially expressed genes involved in the biosynthesis of iridoids between root samples at various growth stages (SP2/SP1; SP3/SP1) and between leaf and root samples (HF/SP). HF: leaf samples from Huaifeng cultivar; SP3: 2 months after sprouting root (root samples); SP2: 1 month after sprouting root (root samples); SP1: 15–20 days after sprouting root (root samples). (B) The phylogenetic tree showing a total of 116 terpene synthase (TPS) with the different TPS subfamilies labeled. TPSs are highlighted in orange while *A. thaliana* TPSs are highlighted in black. (C) The phylogenetic tree showing a total of 191 UDP-dependent glycosyltransferases (UGTs) with the different UGT subfamilies labeled. *R. glutinosa* UGTs are highlighted in red while *A. thaliana* UGTs are highlighted in black. DMAPP: dimethylallyl diphosphate; DXP: 1-deoxy-d-xylulose 5-phosphate; GGPP: geranylgeranyl diphosphate; FPP: farnesyl diphosphate; GPP: geranyl diphosphate; HMBPP: 1-Hydroxy-2-methyl-2-butenyl-4 diphosphate; IPP: ispentenyl diphosphate; MEP: 2-C-methyl-d-erythritol 4-phosphate; MVA: mevalonic acid; G10H: geraniol 8-hydroxylase; 10HGO: 10-hydroxygeraniol oxidoreductase; IS: iridoid synthase; 7-DLS/CYP76A26: 7-deoxyloganetic acid synthase; 7-DLH:7-deoxyloganic acid hydroxylase; 7-DLGT: 7-deoxyloganetic acid glucosyltransferase; LAMT: loganic acid methyltransferase; SLS: secologanin synthase; STR: strictosidine synthase; DXS: 1-deoxy-D-xylulose-5-phosphate synthase; IDI: isopentenyl diphosphate isomerase; DXR: 1-deoxy-D-xylulose 5-phosphate reductoisomerase; GES: geraniol synthase; UGD: UDP-glucuronic acid decarboxylase; HMGR: 3-hydroxy-3-methylglutaryl-CoA synthase; GPS: geranyl diphosphate synthase; GGPS: geranylgeranyl pyrophosphate synthase; FPPS: farnesyl diphosphate synthase; HDR: 4-hydroxy-3-methylbut-2-en-1-yl diphosphate reductase; CPR: cytochrome P450 reductase; CPM: cytochrome *P*-450 monooxygenase; ALDH: aldehyde dehydrogenase; UPD: uroporphyrinogen decarboxylase; F3H: flavanone 3-dioxygenase; SQLE: squalene monooxygenase. (For interpretation of the references to colour in this figure legend, the reader is referred to the web version of this article.)
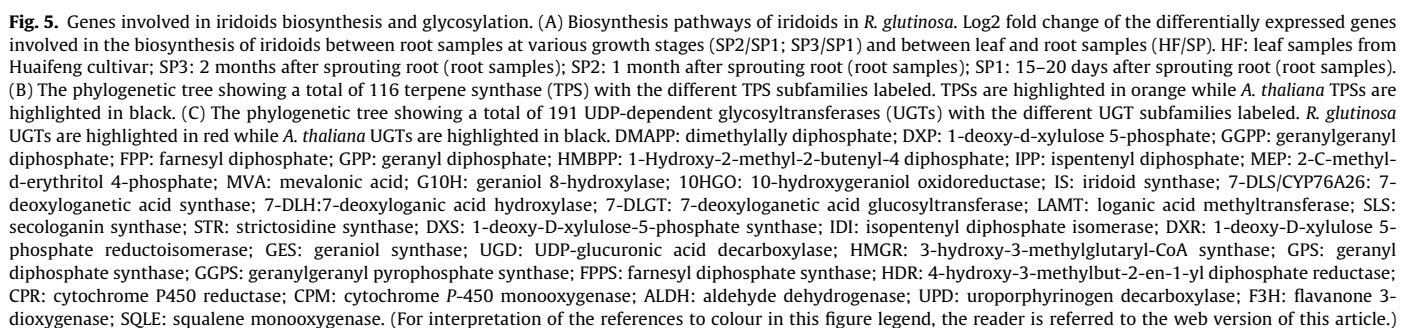
4. Conclusions

We employed a hybrid sequencing approach to resolve the large and highly complex genome of the potent medicinal plant *R. glutinosa*. The newly generated reference genome sequence of *R. glutinosa* increases the genomic resources in the Lamiales order. With the diversity of plant species with special medicinal attributes in the Lamiales order, we anticipate that our results will be cardinal for comparative genomics studies to improve our understanding of the metabolic pathways of specialized bioactive molecules. We provide a strong molecular evidence for the placement of *R. glutinosa* in the Orobanchaceae, a family dominated by parasitic plants. Lineage specific expansion of gene families involved in terpenoid biosynthesis and their preferential expression in root tissue may have contributed to the diversity and enrichment of iridoids in *R. glutinosa* root. Altogether, the released genomic resources of *R. glutinosa* will be essential for gene functional characterization and molecular breeding of high-yielding cultivars.

Author contribution

Ligang Ma and Chi Song: Designed, executed the experiment, performed bioinformatics analysis and drafted the manuscript.

Chengming Dong, Xiaolan Wang, Yan Niu and Xiaoke Zheng: Executed the experiment and contributed in data analysis and interpretation. Weisheng Feng and Shilin Chen: Conceived, and supervised the study; provided the plant materials, financial support and revised the first drafts. All authors have read and approved the final version of this manuscript.

7. Data availability

Rhemannia glutinosa genome assembly sequences have been deposited at the NCBI GenBank under BioProject PRJNA631301

and BioSample Accession SAMN15052190. Raw data of RNAseq used in the present study have been deposited at the NCBI Gen-Bank and the details of the SRA accession numbers are presented in Table S3.

Declaration of Competing Interest

The authors declare that they have no known competing financial interests or personal relationships that could have appeared to influence the work reported in this paper.

Acknowledgement

Not applicable.

Appendix A. Supplementary data

Supplementary data to this article can be found online at https://doi.org/10.1016/j.csbj.2021.07.006.

References

[1] Dixon RA, Strack D. Phytochemistry meets genome analysis, and beyond. Phytochemistry 2003;62(6):815–6.

[2] Chakraborty P. Herbal genomics as tools for dissecting new metabolic pathways of unexplored medicinal plants and drug discovery. Biochim Open 2018;6:9–16.

[3] Liu Y, Dong L, Luo H, Hao Z, Wang Y, Zhang C, et al. Chemical constituents from root tubers of *Rehmannia glutinosa*. Chin Tradit Herb Drugs 2014;45:16–22.

[4] Zhang R-X, Li M-X, Jia Z-P. *Rehmannia glutinosa*: Review of botany, chemistry and pharmacology. J Ethnopharmacol 2008;117(2):199–214.

[5] Zhang X, Zhang A, Jiang Bo, Bao Y, Wang J, An L. Further pharmacological evidence of the neuroprotective effect of catalpol from *Rehmannia glutinosa*. Phytomedicine 2008;15(6-7):484–90.

[6] Gong W et al. *Rehmannia glutinosa* Libosch Extracts Prevent Bone Loss and Architectural Deterioration and Enhance Osteoblastic Bone Formation by Regulating the IGF-1/PI3K/mTOR Pathway in Streptozotocin-Induced Diabetic Rats. Int J Mol Sci 2019;20:3964.

[7] Yuan Y, Kang N, Li Q, Zhang Y, Liu Y, Tan P. Study of the Effect of Neutral Polysaccharides from *Rehmannia glutinosa* on Lifespan of *Caenorhabditis elegans*. Molecules 2019;24(24):4592. https://doi.org/10.3390/molecules24244592.

[8] Shen X et al. Effects of total saponins extracted from leaves of Rehmannia on accelerated nephrotoxic nephritis induced by rabbit IgG in rat. Chin J Exp Tradit Med Form 2010;16:179–81.

[9] Liu C-L, Cheng L, Kwok H-F, Ko C-H, Lau T-W, Koon C-M, et al. Bioassay-guided isolation of norviburtinal from the root of *Rehmannia glutinosa*, exhibited angiogenesis effect in zebrafish embryo model. J Ethnopharmacol 2011;137(3):1323–7.

[10] Hong L, Guo Z, Huang K, Wei S, Liu Bo, Meng S, et al. Ethnobotanical study on medicinal plants used by Maonan people in China. J Ethnobiol Ethnomed 2015;11(1). https://doi.org/10.1186/s13002-015-0019-1.

[11] Li M, Wang X, Zheng X, Wang J, Zhao W, Song K, et al. A new ionone glycoside and three new rhemaneolignans from the roots of *Rehmannia glutinosa*. Molecules 2015;20(8):15192–201.

[12] Li M, Wang X, Zhang Z, Zhang J, Zhao X, Zheng X, et al. Three new alkaloids and a new iridoid glycoside from the roots of *Rehmannia glutinosa*. Phytochem Lett 2017;21:157–62.

[13] Sun P, Song S, Zhou L, Zhang B, Qi J, Li X. Transcriptome analysis reveals putative genes involved in iridoid biosynthesis in *Rehmannia glutinosa*. Int J Mol Sci 2012;13(12):13748–63.

[14] Zhou Y, Wang X, Wang W, Duan HD. *novo* transcriptome sequencing-based discovery and expression analyses of verbascoside biosynthesis-associated genes in *Rehmannia glutinosa* tuberous roots. Mol Breed 2016;36:139.

[15] Wang F et al. Transcriptome Analysis of Salicylic Acid Treatment in *Rehmannia glutinosa* Hairy Roots Using RNA-seq Technique for Identification of Genes Involved in Acteoside Biosynthesis. Front Plant Sci 2017;8:787.

[16] Zhi J et al. Molecular Regulation of Catalpol and Acteoside Accumulation in Radial Striation and non-Radial Striation of *Rehmannia glutinosa* Tuberous Root. Int J Mol Sci 2018;19:3751.

[17] Jiao Z, Cheng Y, Wang H, Lei C, Wang GG, Han L. Isolation and characterization of microsatellite loci in *Rehmannia glutinosa* (Scrophulariaceae), a medicinal herb. Appl Plant Sci 2015;3(10):1500054. https://doi.org/10.3732/apps.1500054.

[18] Oxelman B, Kornhall P, Olmstead RG, Bremer B. Further disintegration of Scrophulariaceae. Taxon 2005;54(2):411–25.

[19] A.H. Wortley P.J. Rudall D.J. Harris R.W. Scotland P. Linder How Much Data are Needed to Resolve a Difficult Phylogeny? 54 5 2005 2005 697 709.

[20] The Angiosperm Phylogeny Group. An update of the Angiosperm Phylogeny Group classification for the orders and families of flowering plants: APG IV. Bot J Linn Soc 2016;181:1–20.

[21] Zeng S, Zhou T, Han K, Yang Y, Zhao J, Liu Z-L. The Complete Chloroplast Genome Sequences of Six Rehmannia Species. Genes 2017;8(3):103. https://doi.org/10.3390/genes8030103.

[22] Hao DC, Xiao PG. Genomics and Evolution in Traditional Medicinal Plants: Road to a Healthier Life. Evolutionary Bioinformatics 2015;11:197–212.

[23] Ibarra-Laclette E, Lyons E, Hernández-Guzmán G, Pérez-Torres CA, Carretero-Paulet L, Chang T-H, et al. Architecture and evolution of a minute plant genome. Nature 2013;498(7452):94–8.

[24] Wang L, Yu S, Tong C, Zhao Y, Liu Y, Song C, et al. Genome sequencing of the high oil crop sesame provides insight into oil biosynthesis. Genome Biol 2014;15(2):R39. https://doi.org/10.1186/gb-2014-15-2-r39.

[25] Cruz F, Julca I, Gómez-Garrido J, Loska D, Marcet-Houben M, Cano E, et al. Genome sequence of the olive tree. *Olea europaea Gigascience* 2016;5(1). https://doi.org/10.1186/s13742-016-0134-5.

[26] Unver T et al. Wild olive genome and oil biosynthesis. Proc Natl Acad Sci 2017;114:E9413–22.

[27] A.-X. Dong H.-B. Xin Z.-J. Li H. Liu Y.-Q. Sun S. Nie et al. High-quality assembly of the reference genome for scarlet sage, Salvia splendens, an economically important ornamental plant 7 7 2018 2018 10.1093/gigascience/giy068.

[28] Li X, Feng T, Randle C, Schneeweiss GM. Phylogenetic Relationships in Orobanchaceae Inferred From Low-Copy Nuclear Genes: Consolidation of Major Clades and Identification of a Novel Position of the Non-photosynthetic Orobanche Clade Sister to All Other Parasitic Orobanchaceae. Front Plant Sci 2019;10:902.

[29] Jiao W-B, Schneeberger K. The impact of third generation genomic technologies on plant genome assembly. Curr Opin Plant Biol 2017;36:64–70.

[30] Amarasinghe SL et al. Opportunities and challenges in long-read sequencing data analysis. Genome Biol 2020;21:30.

[31] Doyle JJ, Doyle JL. A rapid DNA isolation procedure for small quantities of fresh leaf tissue. Phytochem Bull 1987;19:11–5.

[32] Song C, Liu Y, Song A, Dong G, Zhao H, Sun W, et al. The Chrysanthemum nankingense Genome Provides Insights into the Evolution and Diversification of Chrysanthemum Flowers and Medicinal Traits. Molecular Plant 2018;11(12):1482–91.

[33] A. Dobin C.A. Davis F. Schlesinger J. Drenkow C. Zaleski S. Jha et al. STAR: ultrafast universal RNA-seq aligner 29 1 2013 2013 15 21.

[34] Li B, Dewey CN. RSEM: accurate transcript quantification from RNA-Seq data with or without a reference genome. BMC Bioinf 2011;12:323.

[35] Manekar SC, Sathe SR. A benchmark study of k-mer counting methods for high-throughput sequencing. GigaScience 2018;7:giy125.

[36] Liu B et al. Estimation of genomic characteristics by analyzing k-mer frequency in *de novo* genome projects. Quantitative Biology 2013;35:62–7.

[37] Ruan J, Li H. Fast and accurate long-read assembly with wtdbg2. Nat Methods 2020;17:155–8.

[38] Roach MJ, Schmidt SA, Borneman AR. Purge Haplotigs: allelic contig reassignment for third-gen diploid genome assemblies. BMC Bioinf 2018;19:460.

[39] Ramani V, Cusanovich DA, Hause RJ, Ma W, Qiu R, Deng X, et al. Mapping 3D genome architecture through in situ DNase Hi-C. Nat Protoc 2016;11(11):2104–21.

[40] Zhang X, Zhang S, Zhao QM, R.,, Tang, H.. Assembly of allele-aware, chromosomal-scale autopolyploid genomes based on Hi-C data. Nat Plants 2019;5:833–45.

[41] Dudchenko O et al. *De novo* assembly of the genome using Hi-C yields chromosome-length scaffolds. Science 2017;356:92–5.

[42] Durand NC, Robinson JT, Shamim MS, Machol I, Mesirov JP, Lander ES, et al. Juicebox Provides a Visualization System for Hi-C Contact Maps with Unlimited Zoom. Cell Syst 2016;3(1):99–101.

[43] Cantarel BL, Korf I, Robb SMC, Parra G, Ross E, Moore B, et al. MAKER: an easy to-use annotation pipeline designed for emerging model organism genomes. Genome Res 2008;18(1):188–96.

[44] Stanke M, Keller O, Gunduz I, Hayes A, Waack S, Morgenstern B. AUGUSTUS: ab initio prediction of alternative transcripts. Nucleic Acids Res 2006;34(Web Server):W435–9.

[45] Altschul SF, Gish W, Miller W, Myers EW, Lipman DJ. Basic local alignment search tool. J Mol Biol 1990;215(3):403–10.

[46] Grabherr MG et al. Full-length transcriptome assembly from RNA-Seq data without a reference genome. Nat Biotech 2011;29:644.

[47] Simão FA, Waterhouse RM, Ioannidis P, Kriventseva EV, Zdobnov EM. BUSCO: assessing genome assembly and annotation completeness with single-copy orthologs. Bioinformatics 2015;31(19):3210–2.

[48] Apweiler R. UniProt: the universal protein knowledgebase. Nucleic Acids Res 2004;32(90001):115D–9D.

[49] Ashburner M et al. Gene Ontology: tool for the unification of biology. Nat Genet 2000;25:25.

[50] Finn RD et al. Pfam: the protein families database. Nucleic Acids Res 2013;42:D222–30.

[51] Kanehisa M. The KEGG resource for deciphering the genome. Nucleic Acids Res 2004;32(90001):277D–80D.

[52] Jones P, Binns D, Chang H-Y, Fraser M, Li W, McAnulla C, et al. InterProScan 5: genome-scale protein function classification. Bioinformatics 2014;30 (9):1236–40.

[53] Deng Y et al. Integrated nr database in protein annotation system and its localization. Comput Eng 2006;32:71–2.

[54] Todd M. Lowe Sean R. Eddy tRNAscan-SE: a program for improved detection of transfer RNA genes in genomic sequence 25 5 1997 1997 955 964.

[55] Karin Lagesen Peter Hallin Einar Andreas Rødland Hans-Henrik Stærfeldt Torbjørn Rognes David W. Ussery RNAmmer: consistent and rapid annotation of ribosomal RNA genes 35 9 2007 2007 3100 3108.

[56] Nawrocki EP, Eddy SR. Infernal 1.1: 100-fold faster RNA homology searches. Bioinformatics 2013;29(22):2933–5.

[57] Li L, Stoeckert CJ, Roos DS. OrthoMCL: identification of ortholog groups for eukaryotic genomes. Genome Res 2003;13:2178–89.

[58] Robert C. Edgar Quality measures for protein alignment benchmarks 38 7 2010 2010 2145 2153.

[59] Alexandros Stamatakis RAxML version 8: a tool for phylogenetic analysis and post-analysis of large phylogenies 30 9 2014 2014 1312 1313.

[60] De Bie T, Cristianini N, Demuth JP, Hahn MW. CAFÉ: a computational tool for the study of gene family evolution. Bioinformatics 2006;22(10):1269–71.

[61] Yang Z. PAML 4: phylogenetic analysis by maximum likelihood. Mol Biol Evol 2007;24(8):1586–91.

[62] Tang H, Bowers JE, Wang X, Ming R, Alam M, Paterson AH. Synteny and collinearity in plant genomes. Science 2008;320(5875):486–8.

[63] Sara El-Gebali Jaina Mistry Alex Bateman Sean R Eddy Aurélien Luciani Simon C Potter et al. The Pfam protein families database in 2019 47 D1 2019 2019 D427 D432.

[64] Finn RD, Clements J, Eddy SR. HMMER web server: interactive sequence similarity searching. Nucleic Acids Res 2011;39(suppl):W29–37.

[65] Ivica Letunic Peer Bork 20 years of the SMART protein domain annotation resource 46 D1 2018 2018 D493 D496.

[66] Feng Chen Dorothea Tholl Jörg Bohlmann Eran Pichersky The family of terpene synthases in plants: a mid-size family of genes for specialized metabolism that is highly diversified throughout the kingdom 66 1 2011 212 229.

[67] Yonekura-Sakakibara K, Hanada K. An evolutionary view of functional diversity in family 1 glycosyltransferases. Plant J 2011;66:182–93.

[68] Jensen SR. Plant iridoids, Their Biosynthesis and Distribution in Angiosperms. In: Harborne JB, Tomas-Barberan FA, editors. Ecological Chemistry and Biochemistry of Plant Terpenoids. UK: Clarendon Press; Oxford; 1991. p. 133–58.

[69] Zhao Q, Yang J, Cui M-Y, Liu J, Fang Y, Yan M, et al. The Reference Genome Sequence of *Scutellaria baicalensis* Provides Insights into the Evolution of Wogonin Biosynthesis. Mol Plant 2019;12(7):935–50.

[70] Du H, Liang C. Assembly of chromosome-scale contigs by efficiently resolving repetitive sequences with long reads. Nat Commun 2019;10:5360.

[71] Mochida K, Sakurai T, Seki H, Yoshida T, Takahagi K, Sawai S, et al. Draft genome assembly and annotation of *Glycyrrhiza uralensis*, a medicinal legume. Plant J 2017;89(2):181–94.

[72] Lonardi S, Muñoz-Amatriaín M, Liang Q, Shu S, Wanamaker SI, Lo S, et al. The genome of cowpea (*Vigna unguiculata* [L.] Walp.). Plant J 2019;98(5):767–82.

[73] Youjun Huang Lihong Xiao Zhongren Zhang Rui Zhang Zhengjia Wang Chunying Huang et al. The genomes of pecan and Chinese hickory provide insights into Carya evolution and nut nutrition 8 5 2019 2019 10.1093/gigascience/giz036.

[74] Mitsutaka Kadota Osamu Nishimura Hisashi Miura Kaori Tanaka Ichiro Hiratani Shigehiro Kuraku Multifaceted Hi-C benchmarking: what makes a difference in chromosome-scale genome scaffolding? 9 1 2020 2020 10.1093/gigascience/giz158.

[75] Xu Z-H. *Rehmannia glutinosa*: Tissue Culture and Its Potential for Improvement. Medicinal and Aromatic Plants I 1988;501–512.

[76] MORGANTE M, DEPAOLI E, RADOVIC S. Transposable elements and the plant pan-genomes. Curr Opin Plant Biol 2007;10(2):149–55.

[77] Lucia Natali Rosa Cossu Elena Barghini Tommaso Giordani Matteo Buti Flavia Mascagni et al. 14 1 2013 686 10.1186/1471-2164-14-686.

[78] Martínez-García PJ, Crepeau MW, Puiu D, Gonzalez-Ibeas D, Whalen J, Stevens KA, et al. The walnut (*Juglans regia*) genome sequence reveals diversity in genes coding for the biosynthesis of non-structural polyphenols. Plant J 2016;87(5):507–32.

[79] Zhang Y et al. Assembly and Annotation of a Draft Genome of the Medicinal Plant *Polygonum cuspidatum*. Front Plant Sci 2019;10:1274.

[80] Sato S et al. The tomato genome sequence provides insights into fleshy fruit evolution. Nature 2012;485:635–41.

[81] Du H et al. Sequencing and *de novo* assembly of a near complete *indica* rice genome. Nat Commun 2017;8:15324.

[82] Michael TP et al. High contiguity *Arabidopsis thaliana* genome assembly with a single nanopore flow cell. Nat Commun 2018;9:541.

[83] Tomoyuki Kado Hideki Innan Tal Dagan Horizontal gene transfer in five parasite plant species in Orobanchaceae 10 12 2018 2018 3196 3210.

[84] McNeal JR, Bennett JR, Wolfe AD, Mathews S. Phylogeny and origins of holoparasitism in Orobanchaceae. Am J Bot 2013;100(5):971–83.

[85] Schneeweiss, G.M. "Phylogenetic relationships and evolutionary trends in Orobanchaceae," in Parasitic Orobanchaceae: Parasitic Mechanisms and Control Strategies, eds D. M. Joel, J. Gressel, and L. J. Musselman (Berlin: Springer), 243–265 (2013).

[86] Yoshida S, Kim S, Wafula EK, Tanskanen J, Kim Y-M, Honaas L, et al. Genome Sequence of *Striga asiatica* Provides Insight into the Evolution of Plant Parasitism. Curr Biol 2019;29(18):3041–3052.e4.

[87] Lespinet O, Wolf YI, Koonin EV, Aravind L. The role of lineage-specific gene family expansion in the evolution of eukaryotes. Genome Res 2002;12:1048–59.

[88] Demuth JP, Hahn MW. The life and death of gene families. BioEssays 2009;31 (1):29–39.

[89] Zhou Y et al. Metabolite accumulation and metabolic network in developing roots of *Rehmannia glutinosa* reveals its root developmental mechanism and quality. Sci Rep 2018;8:14127.

[90] MacKintosh C, Ferrier DEK. Recent advances in understanding the roles of whole genome duplications in evolution. F1000Res 2017;6:1623.

[91] Fishman L, Willis JH, Wu CA, Lee Y-W. Comparative linkage maps suggest that fission, not polyploidy, underlies near-doubling of chromosome number within monkeyflowers (Mimulus; Phrymaceae). Heredity 2014;112:562–8.

[92] Luo YY, Zhang SQ, Suo JZ, Sun DY, Cui XC. Determination of catalpol in rehmannia root by high performance liquid chromatography. Chin Pharm J 1994;29:38–40.

[93] Tundis R, Loizzo MR, Menichini F, Statti GA, Menichini F. Biological and pharmacological activities of iridoids: recent developments. Mini Rev Med Chem 2008;8:399–420.

[94] Bi J, Wang X-bo, Chen L, Hao S, An L-jia, Jiang B, et al. Catalpol protects mesencephalic neurons against MPTP induced neurotoxicity via attenuation of mitochondrial dysfunction and MAO-B activity. Toxicol In Vitro 2008;22 (8):1883–9.

[95] Laule O, Furholz A, Chang HS, Zhu T, Wang X, Heifetz PB, et al. Crosstalk between cytosolic and plastidial pathways of isoprenoid biosynthesis in *Arabidopsis thaliana*. P Nat Acad Sci 2003;100(11):6866–71.

[96] Damtoft Søren. Biosynthesis of catalpol. Phytochemistry 1994;35(5):1187–9.

[97] Jensen SR, Franzyk H, Wallander E. Chemotaxonomy of the Oleaceae: Iridoids as taxonomic markers. Phytochemistry 2002;60:213–31.

[98] Duan H, Liu W, Zeng Y, Jia W, Wang H, Zhou Y. Expression analysis of key enzymes involved in the accumulation of iridoid in *Rehmannia glutinosa*. Plant Omics Journal 2019(12(02):2019):102–8.

[99] Wang Y, Liao D, Qin M, Li X. Simultaneous determination of Catalpol, Aucubin, and Geniposidic acid in different developmental stages of *Rehmannia glutinosa* leaves by high performance liquid chromatography. Journal of Analytical Methods in Chemistry 2016;2016:1–6.

[100] Dossa K, Mmadi MA, Zhou R, Zhang T, Su R, Zhang Y, et al. Depicting the core transcriptome modulating multiple abiotic stresses responses in sesame (*Sesamum indicum* L.). Int J Mol Sci 2019;20(16):3930. https://doi.org/10.3390/ijms20163930.

[101] Degenhardt Jörg, Köllner TG, Gershenzon J. Monoterpene and sesquiterpene synthases and the origin of terpene skeletal diversity in plants. Phytochemistry 2009;70(15-16):1621–37.

[102] Yu J, Hu F, Dossa K, Wang Z, Ke T. Genome-wide analysis of UDP-glycosyltransferase super family in *Brassica rapa* and *Brassica oleracea* reveals its evolutionary history and functional characterization. BMC Genom 2017;18:474.

[103] Yang X et al. Identification of anthocyanin biosynthesis genes in rice pericarp using PCAMP. Plant Biotechnol J 2019;17:1700–2.

[104] Oshio H, Inouye H. Iridoid glycosides of *Rehmannia glutinosa*. Phytochemistry 1982;21(1):133–8.

[105] Mackenzie PI, Owens IS, Burchell B, Bock KW, Bairoch A, Belanger A, et al. The UDP glycosyltransferase gene superfamily: recommended nomenclature update based on evolutionary divergence. Pharmacogenetics 1997;7 (4):255–69.